

In-core fuel management strategy for the basket-fuel-assembly molten salt reactor

Chun Xue^{1,2} · Zhi-Yong Zhu¹ · Hai-Qing Zhang¹ · Jun Lin¹

Received: 23 December 2016/Revised: 11 April 2017/Accepted: 16 April 2017/Published online: 9 August 2017
© Shanghai Institute of Applied Physics, Chinese Academy of Sciences, Chinese Nuclear Society, Science Press China and Springer Nature Singapore Pte Ltd. 2017

Abstract Molten salt reactor, with good economics and inherent reliability, is one of the six types of Generation IV candidate reactors. The Basket-Fuel-Assembly Molten Salt Reactor (BFAMSR) is a new concept design based on fuel assemblies composed of fuel pebbles made of TRISO-coated particles. Four refueling patterns, similar to the fuel management strategy for water reactors, are designed and analyzed for BFAMSR in terms of economy and security. The MCNPX is employed to calculate the parameters, such as the total duration time, cycle length, discharge burnup, total discharge quantity of ^{235}U , total discharge quantity of ^{239}Pu , neutron flux distribution and power distribution. The in-out loading pattern has the highest burnup and duration time, the worst neutron flux and power distribution and the lowest neutron leakage. The out-in pattern possesses the most uniform neutron flux distribution, the lowest burnup and total duration time, and the highest neutron leakage. The out-in partition alternate pattern has slightly higher burnup, longer total duration time and smaller neutron leakage than that of the out-in loading pattern at the cost of sacrificing some neutron flux distribution and power distribution. However, its alternative distribution of fuel

elements cut down the refueling time. The low-leakage pattern is the second highest in burnup, and total duration time, and its neutron flux and power distributions are the second most uniform.

Keywords BFAMSR · Fuel elements · Fuel management strategy · Loading pattern

1 Introduction

The Generation IV reactors include gas-cooled fast reactor (GFR), lead-cooled fast reactor (LFR), molten salt reactor (MSR), sodium-cooled fast reactor (SFR), supercritical-water reactor (SCWR) and very-high-temperature reactor (VHTR) chosen in the Generation IV initiative Forum [1, 2]. As an old concept, the research of MSR began in the 1950s in Oak Ridge National Laboratory (ORNL) [3–6], aimed at online refueling and recycling of nuclear fuel. Solid fuel MSR, a new concept of reactor proposed in the USA in 2010, uses ceramic coated particles as fuel carrier, and takes the advantage of the high heat capacity and thermal conductivity of the molten salt, giving full play to the merit of coated fuel particles. The representative designs include the advanced high-temperature reactor (AHTR) [7, 8] by ORNL and the pebble-bed advanced high-temperature reactor (PB-AHTR) [9] by UC Berkeley. AHTR uses the plate-shaped coated particle fuel elements, whereas PB-AHTR uses fuel pebbles containing TRISO-coated particles to achieve online refueling through movement of fuel pebbles inside molten salt. The project of thorium-based Molten Salt Reactor (TMSR) was initiated by the Chinese Academy of Science in 2011 [10], aiming at building a 2-MW fluid fuel Molten Salt Experiment

This work was supported by the Strategic Priority Program of Chinese Academy of Sciences (No.XDA02030200).

✉ Zhi-Yong Zhu
zhuzhiyong@sinap.ac.cn
Chun Xue
xuechun.1989@163.com

¹ Shanghai Institute of Applied Physics, Chinese Academy of Sciences, Jiading Campus, Shanghai 201800, China

² University of Chinese Academy of Sciences, Beijing 100049, China

Reactor and a 10-MW solid fuel Molten Salt Experiment Reactor. The 10-MW solid fuel TMSR is a pebble-bed reactor similar to the PB-AHTR, to achieve high-temperature heat output for efficient electric and hydrogen production.

Although the nuclear fuel utilization efficiency can be greatly improved through the online refueling benefited from the use of pebble fuel elements, the reactor operation is facing difficulties due to the complex mechanical structure. It is therefore important to establish an efficient loading technology for solid fuel MSR.

We designed a solid fuel MSR by adopting fuel assemblies composed of TRISO fuel pebbles filling inside a container made of C–C composite [11]. This kind of pebble-bed reactor is called as Basket-Fuel-Assembly Molten Salt Reactor (BFAMSR). The BFAMSR enables the utilization of mature fuel loading techniques similar to that of water cooled reactors. To achieve deeper burnups, water reactor fuel loading patterns can be applied directly. The fuel loading patterns for water reactors [12–17] include the in–out loading, out–in loading, out–in partition alternate loading and low-leakage loading patterns. In this paper, we give a detailed analysis of the loading patterns based on the 10-MW BFAMSR.

2 Modeling of BFAMSR for MCNPX simulation

The 10-MW BFAMSR is composed of an active area and the reflector, with a core in radius of 1.6 m and height of 3.2 m. As shown in Fig. 1, both the active area and side reflector are composed of hexagonal blocks. The fuel assembly hexagonal block is 34.73 cm in side width and 2 m in height. It consists of six triangular prism fuel elements or five triangular prism fuel elements and one control rod channel (Fig. 2). Each triangular prism fuel element is composed of a 1-cm-thick triangular prism can made of C/C composite and 99 fuel pebbles. Fuel pebbles are loaded in the triangular prism can with three pebbles

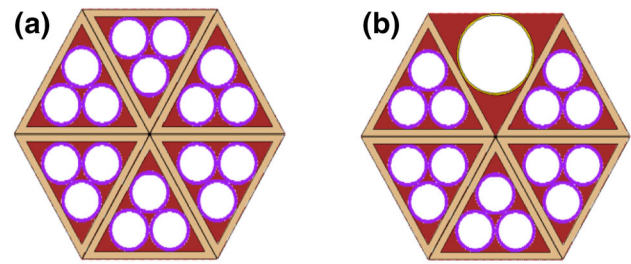


Fig. 2 (Color online) Hexagonal fuel assemblies without **a** and with **b** control rod channel

in each layer. As shown in Fig. 1, the TRISO particles are treated with simple cubic structure distributed in the fuel pebbles. There is a TRISO particle in each small cube, and each TRISO particle is composed of five parts (Fig. 1). Two inner concentric rings of fuel assembly hexagonal blocks form the active area, whose periphery is surrounded by the side reflector. Besides, there is a 60-cm-thick reflector in the bottom and the top of the core, respectively. The 10-MW BFAMSR has 12 control rod channels dispersed in the two concentric rings of the core. The control rods are kept full extracted during the operation of the reactor because we focused only on the neutronic and burnup analysis. All the control rod channels are hollow cylindrical pipe made of carbon material. The geometry data of the 10-MW BFAMSR are given in Table 1, and the material data and temperatures are given in Table 2. As shown, high enriched ^7Li (99.995%) is used.

MCNPX (version 2.5.0) was used in the burnup calculation. It is a Monte Carlo radiation transport calculation code written in Fortran 90 language, prepared by the LANL, which considers almost all particles in various energies [18]. The nuclear data library based on the JEF-2.2 [19, 20] and the database expanded from JENDL3.2, ENDF/B-6.8, DCL-200 and EAF-99 were used in the calculation. The triple heterogeneity of the BFAMSR was treated with the three-dimensional model. Evolution of the

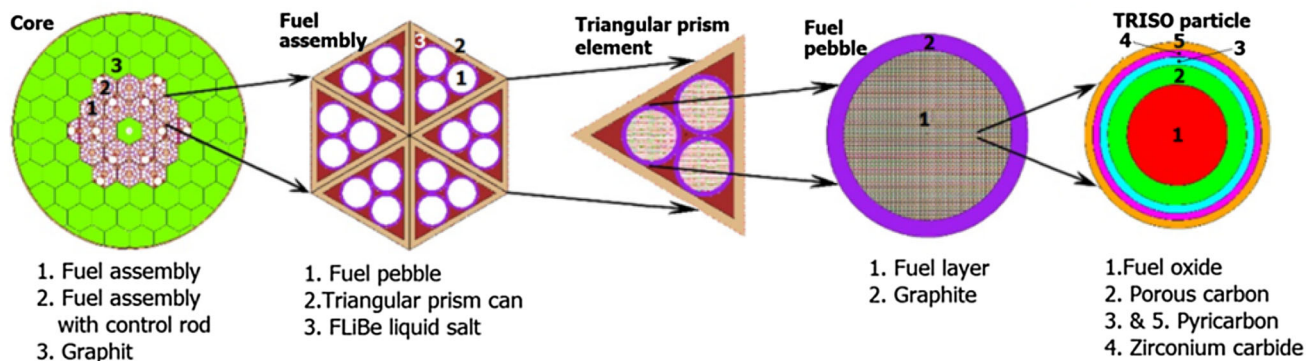


Fig. 1 (Color online) Schematics of the BFAMSR core

Table 1 Geometry data of the 10-MW BFAMRS

Parts	Parameters	Value
Core	Radius (cm)	160
	Height (cm)	320
	Power (MW)	10
Hexagonal fuel assembly	Number: Without control rod	6
	With control rod	12
	Width (cm)	34.73
	Height (cm)	200
	Interstitial gap (cm)	0.05
Control rod channel (in cm)	Radius: inner/outer	5.50/5.75
	Height (cm)	262
Fuel pebble	Number	9504
	Radius (cm)	3
	Volume fraction (%)	48.6
	Packing factor of particles	20
TRISO particles (in cm)	Kernel radius	0.025
	Width: Porous carbon layer	0.009
	Inner pyrocarbon layer	0.004
	SiC layer	0.0035
	Outer pyrocarbon layer	0.004

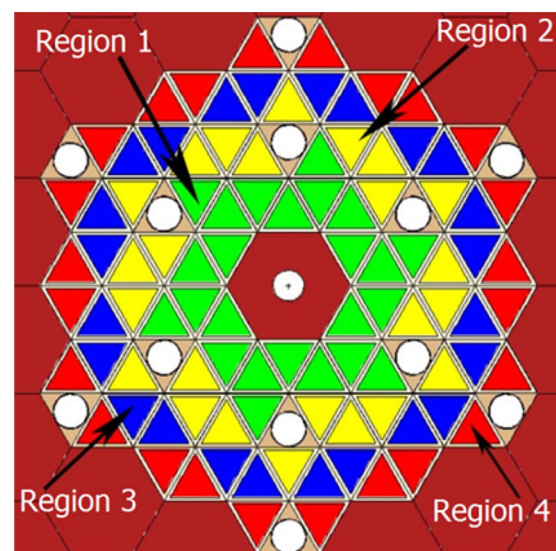
Table 2 Material data of the 10-MW BFAMSR

Material	Atomic percentage (%)	Temperature (°C)	Initial density (g/cm ³)
TRISO kernel	²³⁵ U (5.7267); ²³⁸ U (27.6066); ¹⁶ O (66.6667)	706.1	10.5
TRISO porous graphite	C (100)	700.4	1.1
TRISO pyrocarbon	C (100)	696.4	1.9
TRISO silicon carbide	Si (50); C (50)	695.1	3.18
Graphite in the pebble	C (100)	675.2	1.73
C/C composite	C (100)	615.5	1.9
Reflector	C (100)	615.5	1.76
FLiBe molten salt (99.995% ⁷ Li)	⁶ Li (0.0014); ⁷ Li (28.5700); ⁹ Be (14.2857); ¹⁹ F (57.1429)	615.5	1.9793898

fuel composition with a continuous energy approach was simulated. The burnup by the MCNPX's first run of 10 days was simulated, so as to make the reactor come to the balance of Xe nucleus, and then the burnup was simulated in 30-day steps. Totally 1.25 million particles were simulated in 125 cycles, of which 100 cycles were active [21].

3 Fuel management strategy

The use of fuel assembly in BFAMSR enables the application of relatively mature loading patterns of water reactors, i.e., the in-out loading, out-in loading, out-in partition alternate loading and low-leakage loading patterns. BFAMSR is originally designed for hexagonal assembly replacement, but owing to the small core size of 10-MW BFAMSR, the base unit of fuel replacement in this

**Fig. 3** (Color online) In-out loading pattern

study is taken as the triangular prism fuel elements. The four patterns involved in this study are all 4-batche patterns, and the discharge number of triangular prism fuel

elements in each refueling is 24. For simplicity, the initial U-loading quantity of fuel elements in each region for the four patterns is the same, i.e., the concentration of ^{235}U is

Fig. 4 Approach to the equilibrium, 12 periods in Pattern 1. Region 1 is filled with fresh fuel. The left four columns report the neutron flux ($10^{13} \text{ n cm}^{-2} \text{ s}^{-1}$), the mass (in kg) and the burnups (in GWd/t) at the beginning of the irradiation periods and at the end of the irradiation periods. The last column reports the beginning time, the k_{eff} at the beginning time, the end time and the k_{eff} at the end time of the cycle



17% and TRISO packing factor is 20%. The refueling time is 30 days.

3.1 The analysis of the fuel management strategy

3.1.1 Pattern 1: in-out loading pattern

In Pattern 1, the active area is divided into four regions, i.e., Regions 1, 2, 3 and 4. When refueling, the fresh fuel elements are loaded in Region 1 in the innermost side of the active area, the fuel elements being burned for one cycle in Region 1 are moved to Region 2, the fuel elements being burned for two cycles in Region 2 are moved to Region 3, and the fuel elements being burned for three cycles in Region 3 are moved to Region 4 which is in the outermost side of the active area. The fuel elements being burned for four cycles in Region 4 are discharged. That is to say, after each cycle the burned fuel elements in Region 4 are discharged and the fuel elements from the first to third region are transferred to the next region, respectively, and the new fuel elements are loaded in Region 1 (Fig. 3).

At beginning of the life, all the four regions were loaded with fresh triangular prism fuel elements. At the end of each cycle, the fuel elements were arranged according the ways for refueling mentioned above. Figure 4 detailed some important parameters in each region before and after each cycle. In the left side of Fig. 4, from Column 1 to Column 4 (corresponding to Region 1 to Region 4, respectively), are the neutron flux (10^{-5} eV–20 MeV), quantity of ^{235}U , quantity of ^{239}Pu and burnup in each of the regions. Column 5 of Fig. 4, from top to bottom, gives the beginning time, the effective neutron multiplication factor k_{eff} at the beginning, the end time of the cycle, the k_{eff} at the end of the cycle and duration of the cycle. From Fig. 4, the first cycle lasts for the longest time, up to 1695 days, and the burnups in all the four regions reach more than 85 GWd/t. However, duration for the second cycle reduced to 555 days. That is because in the first cycle all the four regions are filled with fresh fuel elements which give enough excess reactivity for longtime running. But in the second cycle, fresh fuel elements are filled in just Region 1, while the other regions are filled with spent fuel elements burned at least for one cycle. After several times of rise and fall, the cycle time reaches an equilibrium value of 630 days at the 9th cycle. After 12 cycles of operation, a total duration of 8765 days is reached, including $11 \times 30 = 330$ days shutdown time for refueling. After the equilibrium, the time evolution of ^{235}U and ^{239}Pu quantities and the burnups in each of the regions are tending to stable. For Regions 1–4, the equilibrium discharge quantities of ^{235}U is 4.957, 3.333, 2.258 and 1.485 kg, respectively; the equilibrium discharge quantities

of ^{239}Pu is 0.2491, 0.2745, 0.2300 and 0.1697 kg, respectively; and the equilibrium burnups is 54.4, 91.8, 120.5 and 143.4 GWd/t, respectively.

3.1.2 Pattern 2: out-in loading pattern

Contrary to Pattern 1, in the out-in loading pattern, the active area is divided into four regions from the outside to inside. Region 1, where the fresh fuel elements are loaded after each cycle, is in the outermost side of the active area. The ones spent for one cycle are loaded in Region 2. The ones spent for two cycles are loaded in Region 3. And the ones spent for three cycles are loaded in Region 4 which is in the innermost side of the active area. When refueling, the spent fuels in Region 4 are removed, and the fuel elements in the first to third region (Regions 1, 2 and 3) are transferred into the next region (Regions 2, 3 and 4), respectively (Fig. 5).

At beginning of the life, all the four regions were loaded with fresh fuel elements. At the end of each cycle, the ways described in Sect. 3.1.1 were followed for loading, unloading and refueling. The cycle parameters for each region are shown in Fig. 6. Obviously, the parameter change in the first cycle and the corresponding burnups in all the regions are just the same as those in Pattern 1. The second cycle duration decreased greatly to 425 days, rather than 630 days of Pattern 1. The reason is that in Pattern 1 the fresh fuel elements are loaded in the inner side, and due to the high neutron flux in the inner side, the fresh fuel can provide higher excess reactivity (note that the second cycle in Pattern 2 begins with a k_{eff} of 1.087, but it is 1.125 in Pattern 1). Starting from the third cycle, the cycle time varies and comes to an equilibrium value of about 590 days

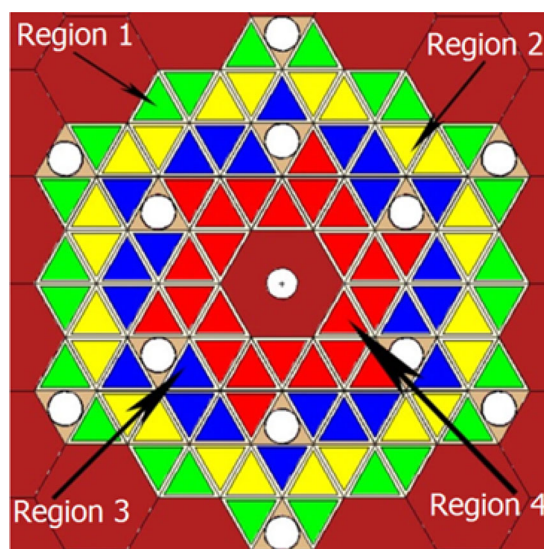
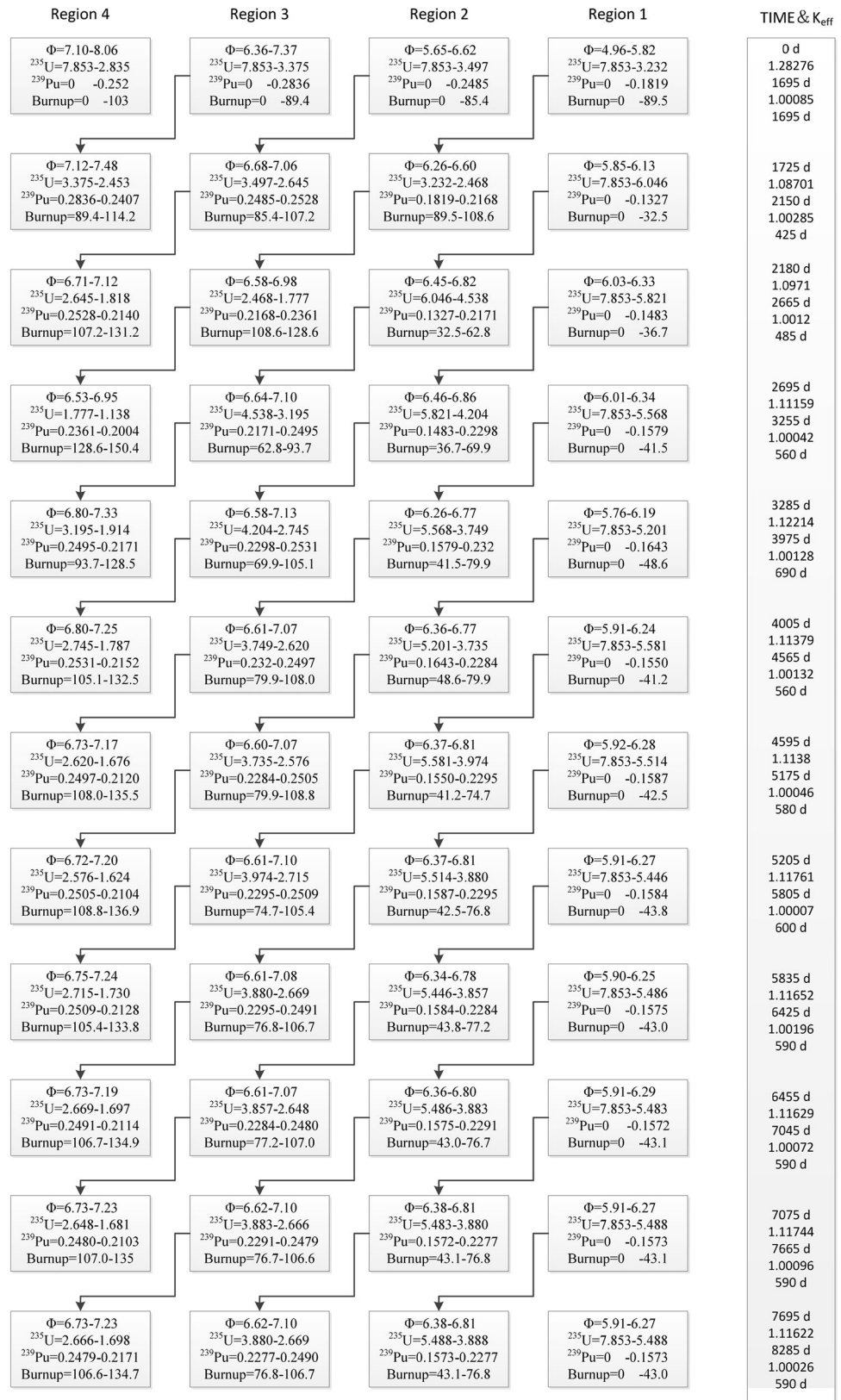


Fig. 5 (Color online) Out-in loading pattern

Fig. 6 Approach to the equilibrium, 12 periods in Pattern 2. Region 1 is filled with fresh fuel. The left four columns report the neutron flux ($10^{13} \text{ n cm}^{-2} \text{ s}^{-1}$), the mass (in kg) and the burnups (in GWd/t) at the beginning of the irradiation periods and at the end of the irradiation periods. The last column reports the beginning time, the k_{eff} at the beginning time, the end time and the k_{eff} at the end time of the cycle



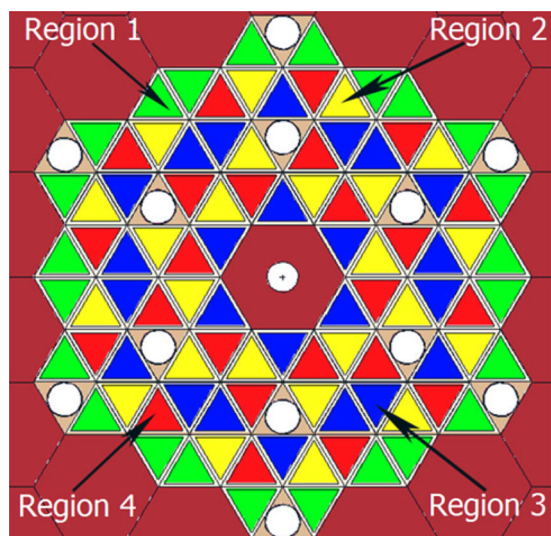


Fig. 7 (Color online) Out-in partition alternate loading pattern

in the 9th cycle. After 12 cycles the total duration time is 8285 days (including shutdown time for refueling) with an equilibrium cycle length of 590 days. For Regions 1–4, the equilibrium quantities of ^{235}U are 5.488, 3.888, 2.669 and 1.698 kg, respectively; the equilibrium quantities of ^{239}Pu are 0.1573, 0.2277, 0.2490 and 0.2171 kg, respectively; and the burnups for the four regions are 43.0, 76.8, 106.7 and 134.7 GWd/t, respectively (Fig. 7).

3.1.3 Pattern 3: out-in partition alternate loading pattern

The out-in partition alternate loading pattern (Pattern 3), a traditional loading pattern for pressurized water reactor, was developed on the basis of Pattern 2. The active area is divided into four regions just the same as Pattern 2, and after each cycle the fresh fuel elements are loaded in Region 1, the outermost of the active area. Different from Pattern 2, in the first refueling, the fuel elements spent for one cycle in Region 1 are loaded in Region 4, with its fuel elements having been discharged. The other regions are kept unchanged. In the second refueling, the ones spent for one cycle in Region 1 are loaded in Region 3, with its fuel elements having been discharged. Again the other regions are kept unchanged. In the third refueling, the ones spent for one cycle in Region 1 are loaded in Region 2, with other regions being kept unchanged. All the other refuelings repeat the above processes: Region 1 → Region 4, Region 1 → Region 3, Region 1 → Region 2 and so on.

At beginning of the life, all the four regions were loaded with fresh fuel elements. At the end of each cycle, the loading, unloading and refueling follow the ways described above. Figure 8 shows the cycle parameters for each region. Obviously, the parameter change in the first cycle is

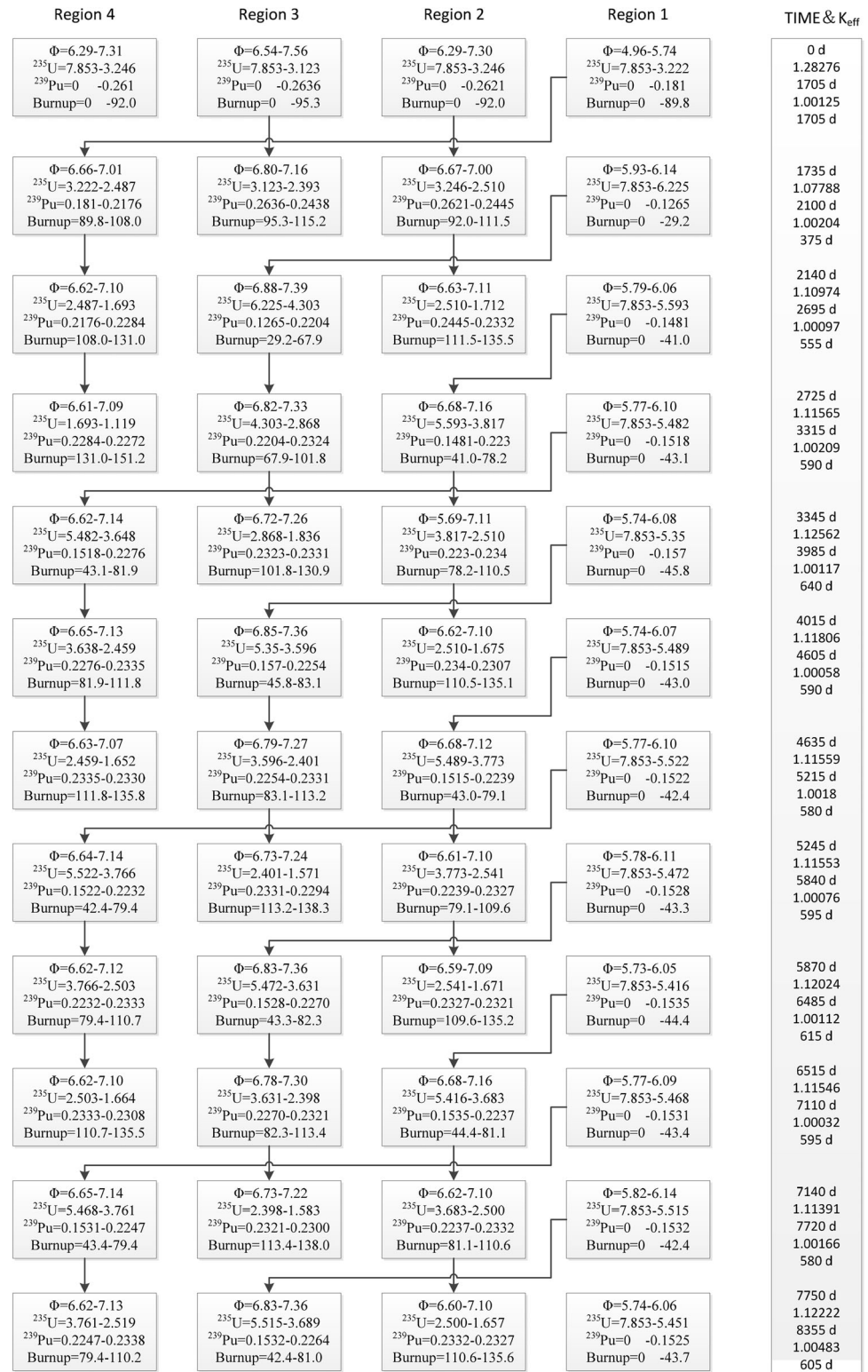
almost the same as those in Patterns 1 and 2, except slight differences caused by the partition alternate arranging mode. Due to the dispersive arrangement of regions in the active area center, the burnups are almost the same in Regions 2–4, about 92.2 GWd/t, but lower in Region 1, 89.8 GWd/t. Duration of Cycle 2 reduced greatly to 375 days, even lower than that in Pattern 2. The reason is the lower total loading quantity of ^{235}U , resulting from the larger discharge quantity of ^{235}U in the first cycle. Then, the cycle time varies and comes to an equilibrium value of 605 days. After 12 cycles the total duration is 8355 days (including shutdown time for refueling). The process to equilibrium is longer than those of the other patterns. This is because that the distribution of the fuel elements in three regions in this pattern is uneven due to the small reactor size. In a larger size reactor, such case would not happen. For Regions 1–4, the equilibrium quantities of ^{235}U are 5.451, 1.657, 3.689 and 2.519 kg, respectively; the equilibrium quantities of ^{239}Pu are 0.1525, 0.2317, 0.2264 and 0.2338 kg, respectively; and the burnups are 43.7, 135.6, 81.0 and 110.2 GWd/t, respectively. The equilibrium discharge quantities of ^{235}U and ^{239}Pu are 1.657 and 0.2317 kg, and the equilibrium discharge burnup is 135.6 GWd/t.

3.1.4 Pattern 4: low-leakage loading pattern

Combining the advantages of Patterns 1–3, the low-leakage loading pattern was developed in the late 1970s, which has been used in the most of the PWR nuclear plants in the world. In Pattern 4, fresh fuel elements are loaded in Region 1, which is in the submargin of the active area after each cycle. The ones spent for one cycle are loaded in the Region 2. The ones spent for two cycles are loaded in the Region 3. And the ones spent for three cycles are loaded in the Region 4. Regions 2–4 are dispersedly alternately arranged (Fig. 9). In refueling, the spent fuels in Region 4 are removed, and the fuel elements in Regions 1–3 are transferred into the next region (Regions 2–4), respectively. That is to say, fuel elements in Region 4 are discharged, and fuel element loadings are Region 3 → Region 4, Region 2 → Region 3, Region 1 → Region 2, and new fuel elements are loaded in Region 1.

At beginning of the life, fresh fuel elements were loaded. At the end of each cycle, the loading, unloading and refueling were done as described previously. Figure 10 details the cycle parameters for each region. Obviously, the parameter change in the first cycle is just the same as that in Patterns 1 and 2, and the corresponding burnup in all the regions is the same. The discharge quantity (3.232 kg) of ^{235}U at the end of the first cycle is

Fig. 8 Approach to the equilibrium, 12 periods in Pattern 3. Region 1 is filled with fresh fuel. The left four columns report the neutron flux (10^{13} n cm⁻² s⁻¹), the mass (in kg) and the burnups (in GWd/t) at the beginning of the irradiation periods and at the end of the irradiation periods. The last column reports the beginning time, the k_{eff} at the beginning time, the end time and the k_{eff} at the end time of the cycle



smaller than Pattern 3 but larger than Pattern 2, and the second cycle time is 395 days. Then, the cycle time varies and finally reaches an equilibrium value of 610 days in Cycle 9. After 12 cycles, the total duration time is 8500 days (including shutdown time for refueling). For

Regions 1–4, the equilibrium quantities of ²³⁵U are 5.566, 3.695, 2.407 and 1.577 kg, respectively; the equilibrium quantities of ²³⁹Pu are 0.2047, 0.2570, 0.2140 and 0.2206 kg, respectively; and the burnups are 41.8, 92.2, 114.8 and 139.3 GWd/t, respectively.

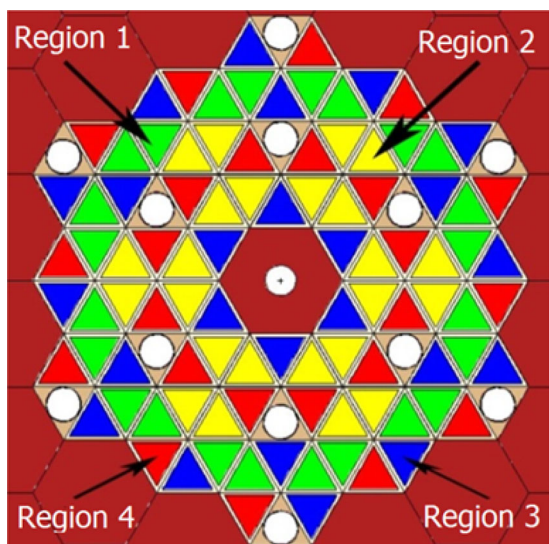


Fig. 9 (Color online) Low-leakage loading pattern

3.2 Analysis of important physical parameters

Table 3 details key physical parameters in the cycle process of the four patterns after reaching equilibrium. They can serve as a measure of the reactor performance. The total duration time, cycle length and the total discharge quantity of ^{235}U can measure the reactor economy. The total discharge quantity of ^{239}Pu and burnups can be used to evaluate the ability of proliferation resistant. Uniformities of the neutron flux distribution and power distribution can be a measure of the reactor security. To evaluate the uniformities, the average neutron flux (f) and the power fraction of each region are compared with the parameters of $\mu = [(f_{\max} - f_{\min})/f_{\max}] \times 100\%$ and $\delta = cp_{\max} - cp_{\min}$, where f_{\max} and f_{\min} are the maximum and minimum values of the average neutron flux in four regions of each pattern, and cp_{\max} and cp_{\min} are the maximum and minimum power fraction among the four regions.

For Pattern 1, the fresh fuel elements are loaded in the innermost side of the active area, which can smooth the burnup and increase the average discharge burnup, and due to loading of fresh elements in the central region, the neutron leakage of the reactor is relatively low, which prolongs the total duration time. From Table 3, Pattern 1 has the largest discharge burnup (143.4 GWd/t), the longest total duration (8755 days) and cycle length (630 days), the lowest total discharge quantity of ^{235}U (20.36 kg) and ^{239}Pu (2.02 kg). These suggest a high economic efficiency of Pattern 1. The main drawback of this pattern is its larger uneven distribution in neutron flux and power, which can greatly limit power level of the reactor. The μ value of Pattern 1 is 45.38%, meaning that the maximum neutron flux is almost double of the minimum neutron flux.

Contrary to Pattern 1, due to loading of fresh fuel elements in the margin of the active area, Pattern 2 features the most uniform neutron flux distribution and power distribution, with $\mu = 12.18$ and $\delta = 14.92\%$, the lowest of all in Table 3. The shortcoming of this pattern is its larger neutron leakage due to that the fresh fuel elements are loaded in the margin of active area. This reduces economics as seen from the shortest total duration of 8285 days, shortest cycle length of 590 days, the decreased burnups of 134.7 GWd/t and the highest total discharge quantity of ^{235}U (22.07 kg).

Pattern 3 is developed on the basis of Pattern 2. Loading the fresh fuel elements in the outermost active area and dispersedly loading the spent fuel elements in other active areas flatten the neutron flux distribution in the entire reactor core and reduce the overall power peak factor. As shown in Table 3, μ and δ are a little higher than those of Pattern 2, but still significantly lower than that of Pattern 1. The refueling is to remove the fuel elements spent for four cycles in an inner regions, fill it with the fuel elements spent for one cycle in an outer region and load the fresh fuel elements in the outermost region, hence no need to move all fuel elements every time and a reduced refueling time. The shortcoming of this pattern is its low discharge burnup.

Pattern 4 combines the advantages of Patterns 1–3. Its advantage is that, due to the deeply burned fuel elements siting in the outermost active area, and the fresh fuel elements being loaded close to the outermost active area, the reactor features a lower neutron flux in the margin of active area and therefore reduces the neutron leakage, improving the neutron utilization and extending the total duration. It has a total duration time of 8500 days, a cycle length of 610 days, a total ^{235}U discharge quantity of 21.09 kg, a total ^{239}Pu discharge quantity of 2.60 kg and a final discharge burnup of 139.3 GWd/t, which are the second best after Pattern 1, but its $\mu = 13.7$ and $\delta = 15.99\%$ are the second the best after Pattern 2, meaning a superiority in safe operation of the reactor.

Figure 11 shows the power fraction taking by each region with the cycles for Patterns 1–4. Figure 12 compares the cycle burnup and the discharge burnup of Patterns 1–4 at each cycle. From Fig. 11, all patterns reach rough equilibrium after nine cycles. Pattern 2 has the most uniform power distribution, followed by Pattern 4. From Fig. 12, Pattern 1 has the highest cycle cycle burnup and discharge burnup, followed by Pattern 4.

3.3 Neutron flux

For the reactor reaching equilibrium, we calculated the average radial neutron flux (ARNF) (from 10^{-5} eV to 20 MeV) at beginning and end of the cycle (BOC and

Fig. 10 Approach to the equilibrium, 12 periods in Pattern 4. Region 1 is filled with fresh fuel. The left four columns report the neutron flux (10^{13} n cm⁻² s⁻¹), the mass (in kg) and the burnups (in GWd/t) at the beginning of the irradiation periods and at the end of the irradiation periods. The last column reports the beginning time, the k_{eff} at the beginning time, the end time and the k_{eff} at the end time of the cycle

Region 4	Region 3	Region 2	Region 1	TIME & k_{eff}
$\Phi=5.84-6.76$ $^{235}\text{U}=7.853-3.232$ $^{239}\text{Pu}=0 -0.2333$ Burnup=0 -91.5	$\Phi=5.82-6.73$ $^{235}\text{U}=7.853-3.056$ $^{239}\text{Pu}=0 -0.2117$ Burnup=0 -95.1	$\Phi=6.77-7.82$ $^{235}\text{U}=7.853-3.131$ $^{239}\text{Pu}=0 -0.2719$ Burnup=0 -95.2	$\Phi=5.65-6.58$ $^{235}\text{U}=7.853-3.500$ $^{239}\text{Pu}=0 -0.2473$ Burnup=0 -85.2	0 d 1.28276 1695 d 1.00067 1695 d
$\Phi=6.45-6.78$ $^{235}\text{U}=3.056-2.312$ $^{239}\text{Pu}=0.2117-0.2157$ Burnup=95.1-114.5	$\Phi=6.45-6.74$ $^{235}\text{U}=3.131-2.353$ $^{239}\text{Pu}=0.2719-0.221$ Burnup=95.2-116.5	$\Phi=7.26-7.66$ $^{235}\text{U}=3.500-2.630$ $^{239}\text{Pu}=0.2473-0.2463$ Burnup=85.2-107.4	$\Phi=6.57-6.87$ $^{235}\text{U}=7.853-6.248$ $^{239}\text{Pu}=0 -0.1636$ Burnup=0 -28.7	1725 d 1.08018 2120 d 1.00221 395 d
$\Phi=6.42-6.83$ $^{235}\text{U}=2.353-1.595$ $^{239}\text{Pu}=0.221-0.2179$ Burnup=116.5-139.4	$\Phi=6.40-6.80$ $^{235}\text{U}=2.630-1.753$ $^{239}\text{Pu}=0.2463-0.2065$ Burnup=107.4-132.9	$\Phi=7.55-8.00$ $^{235}\text{U}=6.248-4.307$ $^{239}\text{Pu}=0.1636-0.2475$ Burnup=28.7-68.5	$\Phi=6.43-6.82$ $^{235}\text{U}=7.853-5.719$ $^{239}\text{Pu}=0 -0.1913$ Burnup=0 -38.8	2150 d 1.11216 2705 d 1.00159 555 d
$\Phi=6.33-6.78$ $^{235}\text{U}=1.753-1.125$ $^{239}\text{Pu}=0.2065-0.212$ Burnup=132.9-154.5	$\Phi=6.38-6.84$ $^{235}\text{U}=4.307-2.790$ $^{239}\text{Pu}=0.2475-0.2108$ Burnup=68.5-104.7	$\Phi=7.39-7.90$ $^{235}\text{U}=5.719-3.753$ $^{239}\text{Pu}=0.1913-0.2507$ Burnup=38.8-80.9	$\Phi=6.37-6.82$ $^{235}\text{U}=7.853-5.515$ $^{239}\text{Pu}=0 -0.1994$ Burnup=0 -42.7	2735 d 1.12092 3360 d 1.0005 625 d
$\Phi=6.33-6.80$ $^{235}\text{U}=2.790-1.791$ $^{239}\text{Pu}=0.2108-0.2175$ Burnup=104.7-132.6	$\Phi=6.33-6.79$ $^{235}\text{U}=3.753-2.386$ $^{239}\text{Pu}=0.2507-0.2097$ Burnup=80.9-115.4	$\Phi=7.32-7.86$ $^{235}\text{U}=5.515-3.575$ $^{239}\text{Pu}=0.1994-0.2523$ Burnup=42.7-84.9	$\Phi=6.35-6.82$ $^{235}\text{U}=7.853-5.456$ $^{239}\text{Pu}=0 -0.2039$ Burnup=0 -43.9	3390 d 1.1274 4040 d 1.00096 650 d
$\Phi=6.36-6.81$ $^{235}\text{U}=2.386-1.580$ $^{239}\text{Pu}=0.2097-0.2137$ Burnup=115.4-139.3	$\Phi=6.38-6.81$ $^{235}\text{U}=3.575-2.352$ $^{239}\text{Pu}=0.2523-0.2087$ Burnup=84.9-116.2	$\Phi=7.36-7.90$ $^{235}\text{U}=5.456-3.657$ $^{239}\text{Pu}=0.2039-0.2501$ Burnup=43.9-83.0	$\Phi=6.41-6.84$ $^{235}\text{U}=7.853-5.614$ $^{239}\text{Pu}=0 -0.1943$ Burnup=0 -40.7	4070 d 1.11565 4660 d 1.0015 590 d
$\Phi=6.36-6.80$ $^{235}\text{U}=2.352-1.542$ $^{239}\text{Pu}=0.2087-0.2139$ Burnup=116.2-140.4	$\Phi=6.37-6.81$ $^{235}\text{U}=3.657-2.386$ $^{239}\text{Pu}=0.2501-0.2084$ Burnup=83.0-115.3	$\Phi=7.39-7.91$ $^{235}\text{U}=5.614-3.735$ $^{239}\text{Pu}=0.1943-0.2502$ Burnup=40.7-81.1	$\Phi=6.41-6.82$ $^{235}\text{U}=7.853-5.573$ $^{239}\text{Pu}=0 -0.1973$ Burnup=0 -41.5	4690 d 1.1207 5295 d 1.00119 605 d
$\Phi=6.36-6.81$ $^{235}\text{U}=2.386-1.568$ $^{239}\text{Pu}=0.2084-0.2140$ Burnup=115.3-140.0	$\Phi=6.37-6.82$ $^{235}\text{U}=3.735-2.443$ $^{239}\text{Pu}=0.2502-0.2096$ Burnup=81.1-114.2	$\Phi=7.37-7.92$ $^{235}\text{U}=5.573-3.711$ $^{239}\text{Pu}=0.1973-0.2497$ Burnup=41.5-82.3	$\Phi=6.39-6.83$ $^{235}\text{U}=7.853-5.583$ $^{239}\text{Pu}=0 -0.1967$ Burnup=0 -42.1	5325 d 1.12104 5940 d 1.00185 615 d
$\Phi=6.35-6.80$ $^{235}\text{U}=2.443-1.602$ $^{239}\text{Pu}=0.2096-0.2140$ Burnup=114.2-138.9	$\Phi=6.36-6.81$ $^{235}\text{U}=3.711-2.419$ $^{239}\text{Pu}=0.2497-0.2092$ Burnup=82.3-114.9	$\Phi=7.39-7.90$ $^{235}\text{U}=5.583-3.709$ $^{239}\text{Pu}=0.1967-0.2503$ Burnup=42.1-82.6	$\Phi=6.38-6.81$ $^{235}\text{U}=7.853-5.570$ $^{239}\text{Pu}=0 -0.1978$ Burnup=0 -41.7	5970 d 1.12343 6580 d 1.00305 610 d
$\Phi=6.34-6.80$ $^{235}\text{U}=2.419-1.585$ $^{239}\text{Pu}=0.2140-0.2150$ Burnup=114.9-139.6	$\Phi=6.37-6.81$ $^{235}\text{U}=3.709-2.417$ $^{239}\text{Pu}=0.2503-0.2088$ Burnup=82.6-115.3	$\Phi=7.38-7.90$ $^{235}\text{U}=5.570-3.697$ $^{239}\text{Pu}=0.1978-0.2517$ Burnup=41.7-82.1	$\Phi=6.38-6.81$ $^{235}\text{U}=7.853-5.566$ $^{239}\text{Pu}=0 -0.1977$ Burnup=0 -41.7	6610 d 1.12039 7220 d 1.00248 610 d
$\Phi=6.34-6.80$ $^{235}\text{U}=2.417-1.583$ $^{239}\text{Pu}=0.2088-0.2148$ Burnup=115.3-140.0	$\Phi=6.37-6.81$ $^{235}\text{U}=3.697-2.407$ $^{239}\text{Pu}=0.2517-0.2090$ Burnup=82.1-114.7	$\Phi=7.38-7.90$ $^{235}\text{U}=5.566-3.696$ $^{239}\text{Pu}=0.1977-0.2506$ Burnup=41.7-82.2	$\Phi=6.38-6.81$ $^{235}\text{U}=7.853-5.565$ $^{239}\text{Pu}=0 -0.1970$ Burnup=0 -41.7	7250 d 1.12128 7860 d 1.00172 610 d
$\Phi=6.35-6.79$ $^{235}\text{U}=2.407-1.577$ $^{239}\text{Pu}=0.2090-0.2206$ Burnup=114.7-139.3	$\Phi=6.36-6.79$ $^{235}\text{U}=3.696-2.407$ $^{239}\text{Pu}=0.2506-0.214$ Burnup=82.2-114.8	$\Phi=7.36-7.90$ $^{235}\text{U}=5.565-3.695$ $^{239}\text{Pu}=0.1970-0.2570$ Burnup=41.7-82.2	$\Phi=6.39-6.81$ $^{235}\text{U}=7.853-5.566$ $^{239}\text{Pu}=0 -0.2047$ Burnup=0 -41.8	7890 d 1.12022 8500 d 1.00237 610 d

EOC) in the active area. As shown in Fig. 13, in the active area of $R < 60$ cm, Pattern 1 has the steepest curve, indicating a very uneven flux distribution, while Pattern 2 has

the most uniform flux distribution. Table 4 compares the neutron flux (Φ) at $R = 10$ cm and $R = 60$ cm at BOC and EOC for Patterns 1–4. The ratio between them, $\Phi(60)/$

Table 3 Important physical parameters of four patterns after reaching equilibrium

Items	Pattern 1	Pattern 2	Pattern 3	Pattern 4
Total time (d)	8755	8285	8355	8500
Cycle length (d)	630	590	605	610
Total discharge quantity of ²³⁵ U (kg)	20.36	22.07	21.78	21.09
Total discharge quantity of ²³⁹ Pu (kg)	2.02	2.61	2.82	2.60
μ (%)	45.38	12.18	15.96	13.72
δ (%)	25.5	14.92	16.2	15.99
Discharge burnup (GWd/t)	143.4	134.7	135.6	139.3

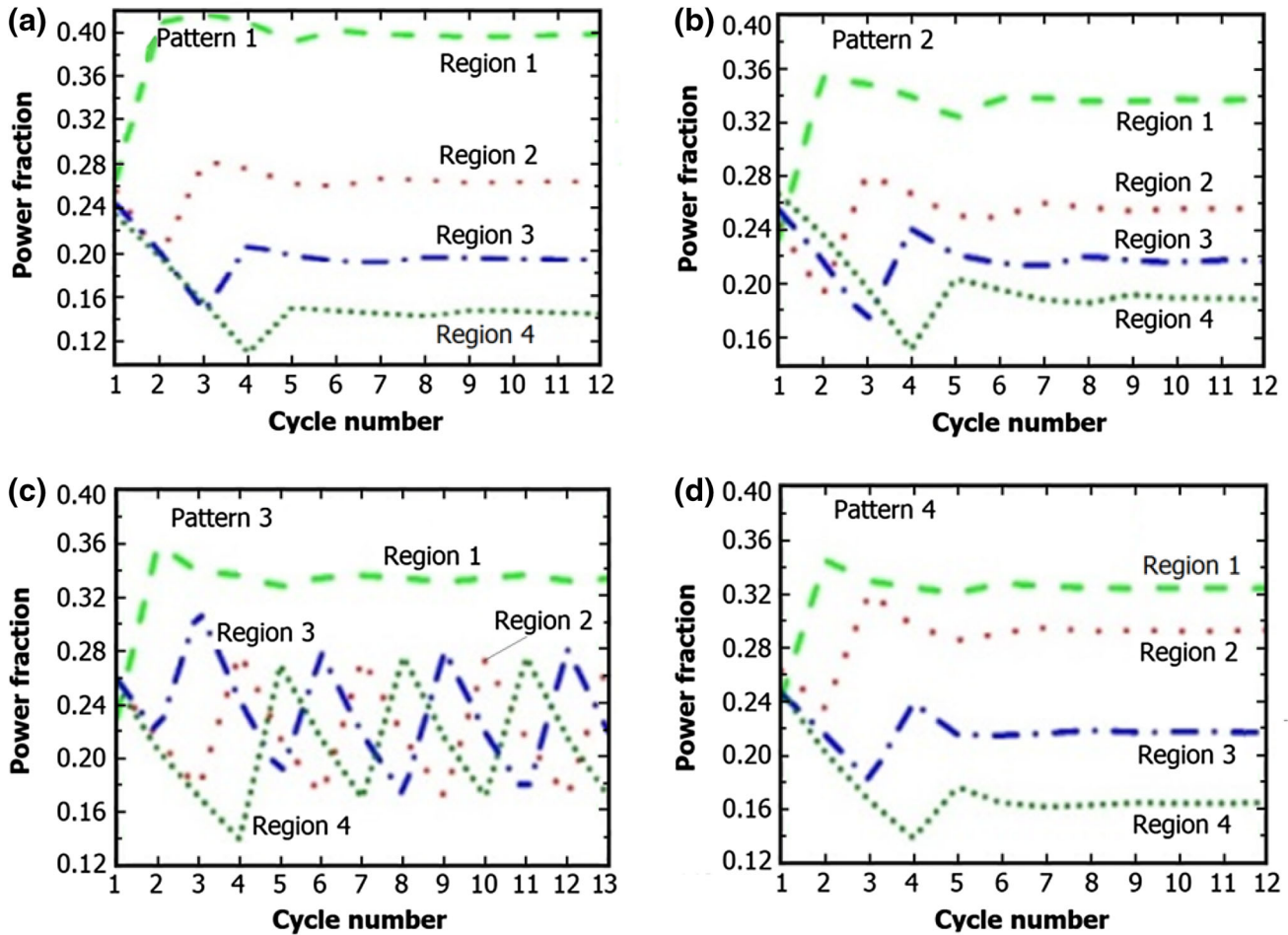


Fig. 11 (Color online) Power fraction in Regions 1–4 for Patterns 1–4 during the first 12 periods of running

$\Phi(10)$, is used to characterize the uniformity of ARNF. Pattern 1 has the smallest ratio, revealing that the neutron flux distribution is of the most uneven one. On the contrary, Pattern 2 has the largest ratio, close to 1, meaning that the neutron flux distribution is very uniform. The ratios for Patterns 3 and 4 are about 0.8, indicating that their neutron flux distribution is better than that of Pattern 1.

The region of $R > 80$ cm in Fig. 13 belongs to the reflector region, where the neutron flux can be used to understand the extent of the neutron leakage. Table 5 details the neutron flux at $R = 80$ cm and $R = 100$ cm for

Patterns 1–4 and the average neutron flux in the range of $0 < R < 60$ cm. Pattern 1 has the lowest neutron leakage, followed by Patterns 4, 3 and 2.

4 Conclusion

The use of Basket-Fuel-Assembly in Molten Salt Reactor enables the utilization of mature fuel loading techniques similar to that of water cooled reactors. The present work studied the feasibility of four fuel loading

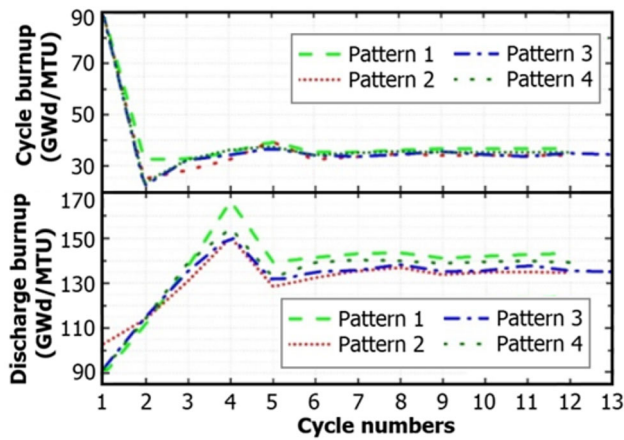


Fig. 12 (Color online) Discharge burnup and cycle burnup of Patterns 1–4 during the first 12 periods of running

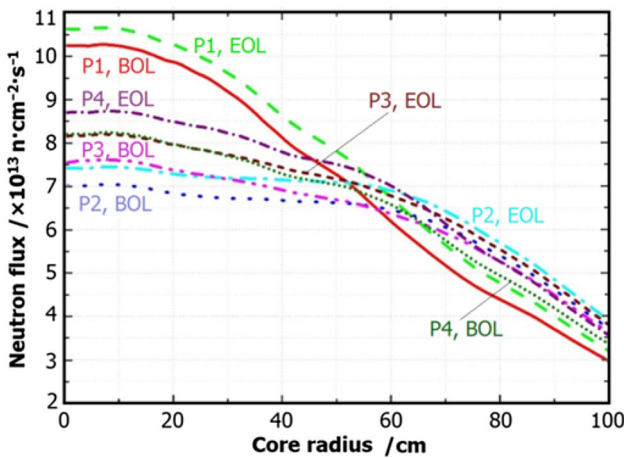


Fig. 13 (Color online) ARNF at BOC and EOC during the first 12 periods of running for the four patterns (P1–P4)

Table 4 Neutron fluxes ($10^{13} \text{ n cm}^{-2} \text{ s}^{-1}$) in the active area at BOC and EOC of Patterns 1–4, for 10 and 60 cm core radius

Neutron flux	$\Phi(60 \text{ cm})$	$\Phi(10 \text{ cm})$	$\Phi(60)/\Phi(10)$
Pattern 1			
BOC	6.13	10.2	0.5995
EOC	6.67	10.6	0.6277
Pattern 2			
BOC	6.44	7.03	0.9168
EOC	6.88	7.43	0.9261
Pattern 3			
BOC	6.34	7.60	0.8349
EOC	6.76	8.18	0.8261
Pattern 4			
BOC	6.54	8.22	0.7958
EOC	6.98	8.72	0.7998

Table 5 ARNF at BOC and EOC of Patterns 1–4 ($10^{13} \text{ n cm}^{-2} \text{ s}^{-1}$), at core radius of up to 100 cm

Neutron flux	$0 < R < 60 \text{ cm}$	$R = 80 \text{ cm}$	$R = 100 \text{ cm}$
Pattern 1			
BOC	8.79	4.35	2.93
EOC	9.24	4.73	3.16
Pattern 2			
BOC	6.77	5.37	3.67
EOC	7.22	5.66	3.86
Pattern 3			
BOC	7.11	5.24	3.58
EOC	7.65	5.50	3.76
Pattern 4			
BOC	7.59	4.90	3.32
EOC	8.09	5.22	3.52

patterns designed for water cooled reactors in BFAMSR, namely in–out loading pattern, out–in loading pattern, out–in partition alternate loading pattern and low-leakage loading pattern, denoted as Patterns 1–4, respectively. The conclusions are as follows:

Pattern 1 has the largest discharge burnup (143.4 GWd/t), the longest cycle length (630 days), and the lowest discharge quantity of ^{235}U (20.36 kg) and discharge quantity (output quantity) of ^{239}Pu (2.02 kg). As far as the economy concerned, Pattern 1 is the best, while as the safety issue concerned, Pattern 1 is limited by its larger uneven power distribution.

Pattern 2 features the most uniform neutron flux distribution and power distribution, but with shortcoming of larger neutron leakage, leading to larger loss of reactivity which affects the burnup and total duration time.

Pattern 3 is developed based on Pattern 2. Benefit from the alternate partition of fuel elements, the discharge burnup and the cycle length are recovered to a certain extent. Meanwhile, in the alternate partition loading pattern not all the fuel elements need to be moved, therefore greatly reducing the time for refueling.

Pattern 4 combines all the advantages of the other three patterns. Loading the fresh fuel elements in the submargin of the active area not only overcomes to a great extent neutron leakage, but also flats the flux distribution and power distribution. Due to the small reactor core size concerned in the present work, the outermost located fuel elements spent for two or three cycles could not stop neutron leakage effectively. But this situation will be much improved in high-power reactors.

The basic rules obtained in analyzing this 10-MW reactor can be applied to large reactors. It is believed that

the study is of great reference value for future design of fuel management for high-power molten salt reactors.

References

- DOE, A technology roadmap for Generation IV nuclear energy systems. Nuclear Energy Research Advisory Committee and the Generation IV International Forum, GIF-002-00
- K. Nagy, D. Lathouwers, C.G.A. T'Joen et al., Steady-state and dynamic behavior of a moderated molten salt reactor. *Ann. Nucl. Energy* **64**, 365–379 (2014). doi:[10.1016/j.anucene.2013.08.009](https://doi.org/10.1016/j.anucene.2013.08.009)
- H.G. MacPherson, The molten salt reactor adventure. *Nucl. Sci. Eng.* **90**, 374–380 (1985). doi:[10.13182/NSE90-374](https://doi.org/10.13182/NSE90-374)
- J. Serp, M. Allibert, O. Benes et al., The molten salt reactor (MSR) in generation IV: overview and perspectives. *Prog. Nucl. Energy* **77**, 308–319 (2014). doi:[10.1016/j.pnucene.2014.02.014](https://doi.org/10.1016/j.pnucene.2014.02.014)
- E.S. Bettis, R.W. Schroeder, G.A. Cristy et al., The aircraft reactor experiment design and construction. *Nucl. Sci. Eng.* **2**(6), 804–825 (1957)
- M.W. Rosenthal, P.R. Kasten, R.B. Briggs, Molten-salt reactors—history, status, and potential. *Nucl. Appl. Technol.* **8**, 107–117 (1970)
- P. Avigni, B. Petrovic, Fuel element and full core thermal-hydraulic analysis of the AHTR for the evaluation of the LOFC transient. *Ann. Nucl. Energy* **64**, 499–510 (2014). doi:[10.1016/j.anucene.2013.05.029](https://doi.org/10.1016/j.anucene.2013.05.029)
- V.K. Varma, D.E. Holcomb, F.J. Peretz et al., AHTR mechanical, structural, and neutronic preconceptual design. ORNL/TM-2012/320, ORNL. doi:[10.2172/1054145](https://doi.org/10.2172/1054145)
- M. Fratoni, E. Greenspan, Neutronic feasibility assessment of liquid salt-cooled pebble bed reactors. *Nucl. Sci. Eng.* **168**(1), 1–22 (2011). doi:[10.13182/NSE10-38](https://doi.org/10.13182/NSE10-38)
- M.H. Jiang, H.J. Xu, Z.M. Dai, Advanced fission energy program-TMSR nuclear energy system. *Bull. Chin. Acad. Sci.* **27**(3), 366–374 (2012). doi:[10.3969/j.issn.1000-3045.2012.03.016](https://doi.org/10.3969/j.issn.1000-3045.2012.03.016). (in Chinese)
- C. Xue, H.Q. Zhang, Z.Y. Zhu et al., Design of fuel assembly for molten-salt-cooled reactors. *Nucl. Tec.* **39**(090602–1), 090602–090608 (2016). doi:[10.11889/j.0253-3219.2016.hjs.39.090602](https://doi.org/10.11889/j.0253-3219.2016.hjs.39.090602). (in Chinese)
- Z.S. Xie, *Nuclear Reactor Physics Analysis* (Xi'an Jiaotong University Press, Xi'an, 2004), pp.253–285. (in Chinese)
- V.N. Bukanov, V.L. Demekhin, A.A. Korennoi, Use of low neutron leakage fuel loads to decrease the radiation load on a VVÉR-1000 vessel. *At. Energy.* **101**(2), 544–548 (2006). doi:[10.1007/s10512-006-0128-y](https://doi.org/10.1007/s10512-006-0128-y)
- A. Talamo, W. Gudowski, Adapting the deep burn in-core fuel management strategy for the gas turbine—modular helium reactor to a uranium–thorium fuel. *Ann. Nucl. Energy* **32**, 1750–1781 (2005). doi:[10.1016/j.anucene.2005.07.002](https://doi.org/10.1016/j.anucene.2005.07.002)
- A. Thakur, B. Singh, P.D. Krishnani, In-core fuel management for AHWR. *Ann. Nucl. Energy* **57**, 47–58 (2013). doi:[10.1016/j.anucene.2013.01.034](https://doi.org/10.1016/j.anucene.2013.01.034)
- N.J. Hill, G.T. Parks, Pressurized water reactor in-core nuclear fuel management by tabu search. *Ann. Nucl. Energy* **75**, 64–71 (2015). doi:[10.1016/j.anucene.2014.07.051](https://doi.org/10.1016/j.anucene.2014.07.051)
- T.J. Downar, A. Sesonske, Light water reactor fuel cycle optimization: theory versus practice. *Adv. Nucl. Sci. Technol.* **20**(20), 71–126 (1988). doi:[10.1007/978-1-4613-9925-4_2](https://doi.org/10.1007/978-1-4613-9925-4_2)
- J.S. Hendricks, G.W. Mckinney, M.L. Fensin, MCNPX 2.6.0 Extensions. LA-UR-08-2216, Los Alamos National Laboratory (2008)
- K. Shibata, O. Iwamoto, T. Nakagawa et al., JENDL-4.0: a new library for nuclear science and engineering. *J. Nucl. Sci. Technol.* **48**, 1–30 (2011). doi:[10.1080/18811248.2011.9711675](https://doi.org/10.1080/18811248.2011.9711675)
- Z.G. Ge, Z.X. Zhao, H.H. Xia et al., The updated version of Chinese evaluated nuclear data library (CENDL-3.1). *J. Korean Phys. Soc.* **59**, 1052–1056 (2011). doi:[10.3938/jkps.59.1052](https://doi.org/10.3938/jkps.59.1052)
- K. Allen, T. Knight, S. Bays, Benchmark of advanced burner test reactor model using MCNPX 2.6.0 and ERANOS 2.1. *Prog. Nucl. Energy* **53**, 633–644 (2011). doi:[10.1016/j.pnucene.2011.01.007](https://doi.org/10.1016/j.pnucene.2011.01.007)